

Adsorption, segregation, and magnetization of a single Mn adatom on the GaAs(110) surfaceJ. X. Cao,^{1,2} X. G. Gong,^{1,3} and R. Q. Wu^{1,4}¹*Interdisciplinary Center of Theoretical Studies, Chinese Academy of Sciences, 100080 Beijing, China*²*Department of Physics, Xiangtan University, 411105, Xiangtan, China*³*Surface Science Laboratory (State Key) and Department of Physics, Fudan University, 200433 Shanghai, China*⁴*Department of Physics and Astronomy, University of California, Irvine, California 92697, USA*

(Received 18 March 2005; revised manuscript received 21 July 2005; published 27 October 2005)

Density functional calculations with a large unit cell have been conducted to investigate adsorption, segregation, and magnetization of Mn monomer on GaAs(110). The Mn adatom is rather mobile along the trench on GaAs(110) with an energy barrier of 0.56 eV. The energy barrier for segregation across the trenches is nevertheless very high, 1.67 eV. The plot of density of states display a wide gap in the majority spin channel, but show plenty of metal-induced gap states in the minority spin channel. The Mn atoms might be “invisible” in scanning tunneling microscope (STM) images taken with small biases, due to the directional p-d hybridization. For example, one will more likely see two bright spots on Mn/GaAs(110), despite the fact there is only one Mn adatom in the system.

DOI: [10.1103/PhysRevB.72.153410](https://doi.org/10.1103/PhysRevB.72.153410)

PACS number(s): 68.35.Dv, 68.37.Ef

Diluted magnetic semiconductors (DMS) offer superior compatibilities to base semiconductors and promise high spin injection rates for spintronics manipulations.^{1–4} However, exploitation of DMS seems still severely hindered by several major complexities. For (Ga,Mn)As, a prototype DMS that has attracted extensive attention in the past decade,⁵ it was found that low temperature annealing procedures are necessary to enhance the Curie temperature, T_c , from 60–80 K for as-grown samples to 110–160 K.^{6,7} Through comparison with experimental results of x ray magnetic circular dichroism (XMCD),⁸ we estimated that about 30% Mn dopants take the interstitial sites in the as-grown (Ga,Mn)As samples^{9,10} and the increase in T_c is primarily caused by the segregation of interstitial Mn toward the surface.¹¹ On the other hand, Mn atoms in the surface region can be converted to substitutional dopants, as was revealed in recent studies through density functional calculations and cross-sectional scanning tunneling microscope (STM) experiments.^{12,13} Understanding adsorption and segregation of magnetic impurities on semiconductor surfaces hence becomes closely relevant to investigations of DMS, and moreover to the design and fabrication of excellent magnetic wires, dots, and interfaces. The growth of (Ga,Mn)As is normally along the (001) orientation. Erwin *et al.*¹⁴ found Mn adatoms tend to funnel into the interstitial site right beneath the GaAs(001) surface. Yet, very few publications can be found for Mn/GaAs(110). GaAs(110) has no surface states in the gap and is hence more suitable for STM explorations. Yakunin *et al.*¹⁵ observed strong anisotropic features of the hole states induced by the Mn acceptors on an *in situ* cleaved (Ga,Mn)As (110) surface. Kitchen *et al.*¹⁶ manipulated and observed the electronic states of Mn adatoms on GaAs(110) surfaces and also found unusual features for the Mn-induced gap states. Here we report results of density functional calculations for Mn monomer on GaAs(110) that are helpful to elucidate the origin of these peculiar wave function features and, furthermore, to investigate the energetics of Mn segregation on this important surface.

In the bulk zinc-blend semiconductors, there are three high symmetric interstitial positions, namely, the two tetrahedral sites, surrounded by four nearest neighboring cations (the T_{Ga} site) or anions (the T_{As} site), and a hexagonal site, surround by six nearest neighbors (three cations and three anions). Edmonds *et al.*¹¹ estimated that the energy barrier governing the diffusion of interstitial Mn in the bulk (Ga,Mn)As is 0.7 ± 0.1 eV. The energy barriers have also been calculated by several other groups and results are still somewhat controversial. Through the full potential linearized augmented plane wave (FLAPW) calculation, Masek *et al.*¹⁷ found that the formation energies are very close for Mn in either the T_{As} or T_{Ga} site. The hexagonal interstitial site, however, is higher in energy by 0.52 eV. In contrast, results obtained from plane wave calculations indicate that T_{Ga} sites is about 0.35 eV higher in energy for a single interstitial Mn and the energy barrier for its diffusion is 0.8 eV.¹¹ Results of our own calculations using the Vienna *ab initio* simulation package (VASP) code are close to Masek's data if the positions of Ga and As atoms are frozen.¹⁸ On the contrary, the total energies for Mn at all three sites are almost the same when the lattice size and atomic positions of GaAs are fully relaxed. In this paper, we report that the Mn monomer migrates along the trench on the GaAs(110) surface with an energy barrier of 0.56 eV. T_{Ga} is the most stable adsorption site while T_{As} is a metastable adsorption site. The magnetic moment of Mn/GaAs(110) is $3.0 \mu_B$. Importantly, Mn induces pronounced resonances in the band gap in the minority spin channel. The wave functions of these gap states are very directional and unusual anisotropic STM images are predicted.

To determine the potential energy surface (PES), we calculated the binding energies of Mn on seven different adsorption sites as shown in Fig. 1. Among these sites III, IV, and VI correspond to the hexagonal positions while V and VII are the T_{As} and T_{Ga} sites in the bulk GaAs, respectively. The projected augmented wave (PAW) approach and the generalized gradient approximation (GGA), implemented in the

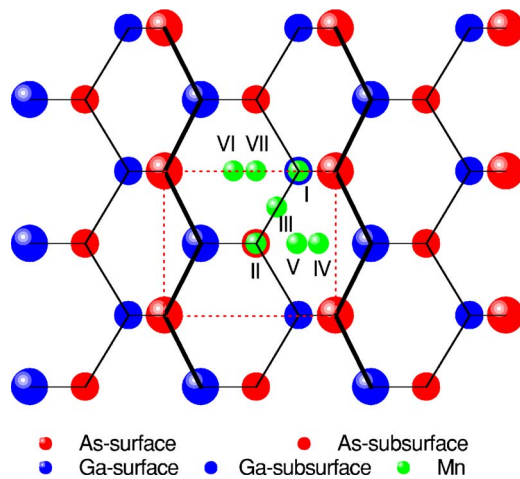


FIG. 1. (Color online) A sketch of the $p(3 \times 3)$ unit cell and adsorption configurations for the simulations of Mn/GaAs(110). The dashed rectangle gives the primitive 2D unit cell for the clean GaAs(110) surface.

VASP code, were used in the present calculations. We modeled the GaAs (110) surface with a slab geometry that contains five GaAs layers and a vacuum of 10.0 Å thick in between. To minimize the remaining size effect due to the use of finite slab, the bottom surface is passivated with a layer of H. In the lateral plane, we used a 3×3 super cell so as to

mimic the environment for a single adsorbate. Energy cutoff of 300 eV was chosen for the plane wave basis expansions. 4×4 special k mesh points in the Brillouin-zone were used to evaluate integrations in the reciprocal space. The vertical position of the Mn adatom is fully relaxed for a given (x, y) position. The positions of Ga and As atoms in the topmost three layers are also fully optimized, whereas those in the two bottom most layers are frozen at their bulk positions. The criterion for structural optimization requires the calculated force on each unconstrained atom smaller than 0.01 eV/Å. Results of multilayer relaxations for the clean GaAs(110) surface from test calculations agree very well with data in the literature, indicating the validity of the present treatment. We found that a large search range should be given to the z coordinate of Mn since local minima are frequently involved when the substrate relaxes simultaneously.

The calculated two-dimensional PES for Mn/GaAs(110) displays a strong spatial anisotropy in Fig. 2. The red line indicates that the apparent segregation path for Mn is along the trench on the GaAs(110) surface. Quantitatively, the total energy increases very steeply away from its minimum at a point close to the T_{Ga} site (slightly shifted toward site VI). To pass through site III toward the metastable T_{As} site (V), the Mn adatom needs to overcome an energy barrier of 0.56 eV. Nevertheless, the energy barrier for the reverse trip is very shallow, only 0.2 eV. In contrast, there is no obvious channel

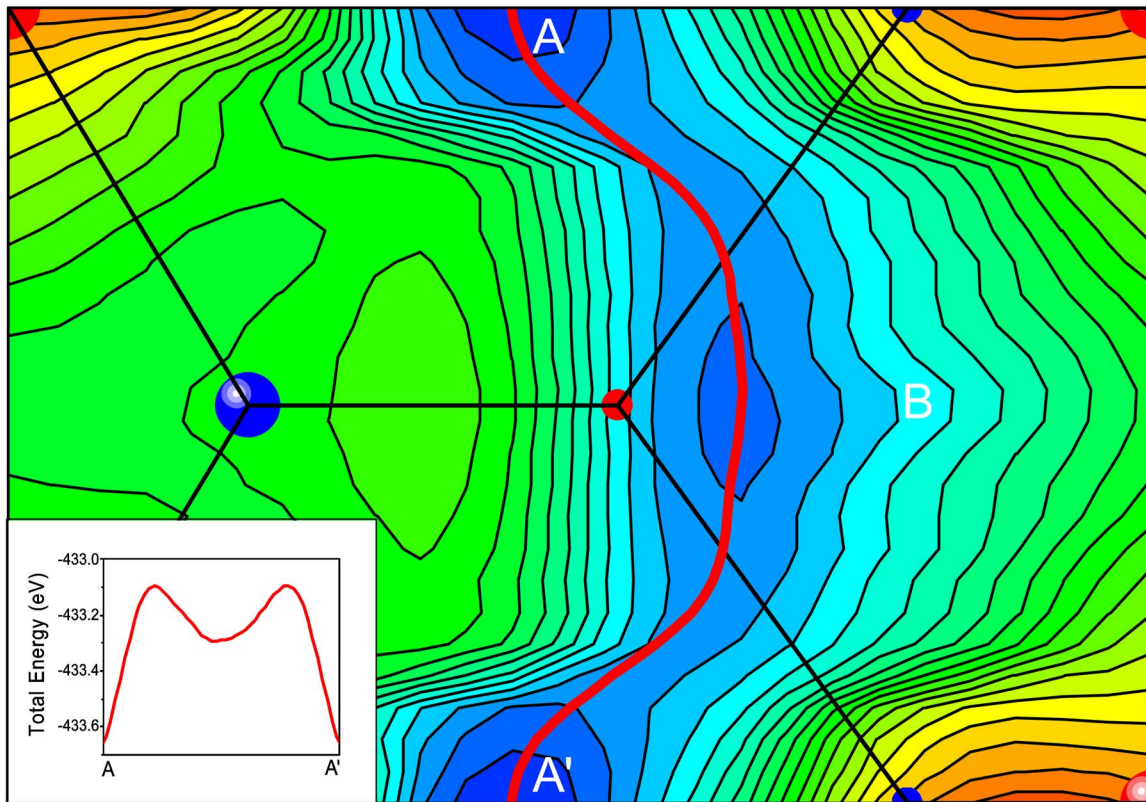


FIG. 2. (Color online) The potential-energy surface for Mn diffusion on GaAs(110). Dark colors indicate higher binding energies whereas light colors represent lower binding energies. The balls and straight black lines give the position of the surface and subsurface Ga and As atoms and the bonds between them. The red (light gray) line shows the minimum energy segregation path and the inset gives the total energy versus the position of Mn along this path.

TABLE I. The z position of Mn [measured from the topmost As layer of the relaxed clean GaAs(110) surface], the nearest Mn-Ga and Mn-As interatomic distances, the total and local magnetic moment as well as the number of electrons integrated in the Mn muffin-tin sphere for different adsorption configurations.

Adsorption site	z (Å)	$d_{\text{Mn-Ga}}$ (Å)	$d_{\text{Mn-As}}$ (Å)	N_{MT} (electron)	M (μ_B)	M_{MT} (μ_B)
I	2.00		2.58	4.99	5.00	4.33
II	0.39	2.36	2.62	5.05	5.00	4.08
III	-0.29	2.45	2.47	5.19	3.00	3.41
IV	-1.03	2.47	2.51	5.23	3.00	3.16
V	-0.66	2.50	2.33	5.28	3.00	3.06
VI	-0.73	2.44	2.46	5.21	3.00	3.27
VII	-0.24	2.57	2.59	5.12	3.00	3.57

for Mn to segregate across the trenches and the smallest energy barrier for such a segregation is as high as 1.67 eV. Therefore, Mn migration on GaAs(110) is one-dimensional at ambient temperature, only along the trench. Although it is expected that the Mn adatom resides mostly on the T_{Ga} site, the small energy barriers make it rather mobile.¹⁹ So far, there is no direct measurement for the segregation barriers on Mn/GaAs(110). Density functional calculations done by Ishii *et al.* found a similar size of energy barriers for migrations of Ga and As along the trench, 0.57 eV.²⁰ The barrier height estimated for Mn impurities in bulk (Ga,Mn)As is somewhat larger, 0.7 ± 0.1 eV, but this value might be affected by the attraction between the interstitial and substitutional Mn.¹¹

On GaAs(001), Erwin *et al.*¹⁴ found two locally stable adsorption positions: 2.0 Å above or below the surface As dimer. The site below the surface is more favorable by 0.8 eV and the barrier between the two sites is only 0.2 eV. Most Mn atoms on the surface should be funneled in to the T_{As} interstitial site right beneath the surface. However, in this study Mn was limited on the plane of As dimer normal to the surface. It is unclear if the energy barriers are different through other pathways. Our calculations for Mn on GaAs(110) revealed a high sensitivity of energy barriers for bulk-to-surface segregations on the shifts of Ga and As atoms in the xy -plane. Besides, the Ga-As bonds on the (110) surface are much stronger than the As-As bonds on the (100) surface. The segregation of Mn in the trench is expected to be the dominant precursor state for substitution and is also very important for studies of bulk-to-surface diffusion on GaAs(110).

Table I presents the optimized z positions of the Mn adatom, the nearest Mn-Ga and Mn-As interatomic distances, the total magnetic moments, and the local magnetic moments along with the number of electrons integrated in the Mn muffin-tin region ($r_{\text{Mn}} = 1.17$ Å). Strikingly, the value of z remains negative except on the unstable sites, I and II (cf. Figs. 1 and 2) indicating that Mn stays below the topmost As layer when it migrates in the trench. The Mn appear to be positively charged on GaAs(110) and show an attractive (repulsive) tendency toward As (Ga). This is manifested by the

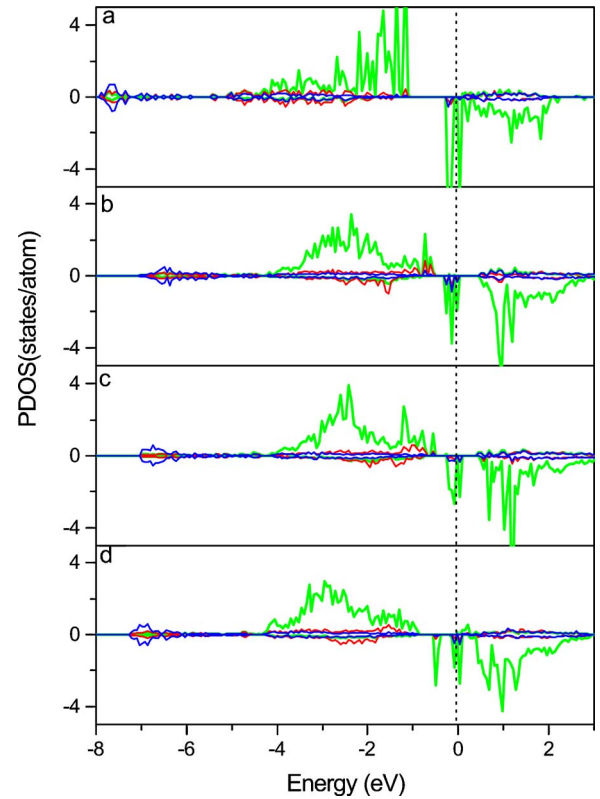


FIG. 3. (Color online) The atom-projected density of states for Mn (green or light lines) and its nearest Ga (blue or dark lines) and As (red or gray lines) neighbors. Results in panels (a), (b), (c), and (d) are for the interstitial Mn in the bulk GaAs (at the T_{Ga} site), Mn adatom on T_{Ga} , T_{As} and hexagonal sites over GaAs(110), respectively. States in the majority and minority spins are separated with positive and negative signs. Zero energy in the horizontal axis indicates the position of the Fermi level.

fact that $d_{\text{Mn-As}}$ is smaller than $d_{\text{Mn-Ga}}$ by 0.17 Å on the T_{As} (or V) site whereas they are almost the same on the T_{Ga} (or VII) site. The total magnetic moment of Mn/GaAs(110) is $3.0 \mu_B$ for low-energy configurations. This value is close to that obtained for an interstitial Mn impurity in the bulk GaAs, $3.1 \mu_B$. However, the contribution in the Mn muffin-tin region, M_{MT} , fluctuates in a wide range. For example, M_{MT} is $3.57 \mu_B$ on the T_{Ga} site but it becomes $3.06 \mu_B$ on the T_{As} site. Moreover, slight changes can be found for the number of electrons in the Mn muffin-tin sphere, N_{MT} , from 5.12 to 5.28 electrons for low-energy configurations. Obviously, the localization and spin polarization of Mn states vary significantly in different adsorption sites.

The projected density of states (PDOS) for the interstitial Mn impurity in the bulk GaAs, Mn adsorbates on GaAs(110) (on T_{Ga} , T_{As} and the hexagonal sites, respectively) are plotted in Fig. 3. Mn adatom induces gap states around E_F in the minority spin channel in all cases, but the lowest d_{yz} state is well separated from other Mn d states in Mn/GaAs(110). Meanwhile, the amplitude of resonances on surrounding Ga and As atoms around E_f is somewhat enhanced, primarily due the shortened $d_{\text{Mn-Ga}}$ and $d_{\text{Mn-As}}$ after relaxations. Although the details of PDOS curves defer from case to case, the Mn d states remain fully occupied in the majority spin

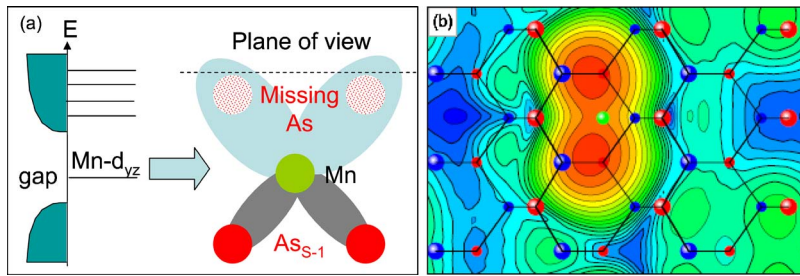


FIG. 4. (Color online) (a) The schematic energy and wave function diagrams of the gap states. (b) The energy-sliced charge densities plotted in a horizontal plane which is 4 Å above the Mn adatom for the T_{Ga} configurations. States only within -0.25 eV to $+0.25$ eV around E_F contribute to the plots.

channel. The Mn adatom is thus 100% spin polarized in the vicinity around E_F .

It is important to examine the wave function features of the gap states so as to understand the adsorbate-substrate interaction. Experimentally, one can observe these gap states on Mn/GaAs(110) through STM with a small bias. For comparison in the future, the energy-sliced charge density (from states within ± 0.25 eV) is plotted in Fig. 4 for the T_{Ga} configurations. As mentioned above, the Mn is almost equally distant from the subsurface Ga and As atoms. The $Mn-d_{yz}$ state hybridizes with As underneath and is lowered in energy. Interestingly, no electron cloud can be found right on the top of Mn. Instead, two distinguished lobes, 4.0 Å apart, can be seen above the subsurface As atoms. One thus sees two bright spots on Mn/GaAs(110) in STM images, even though there is only one Mn adatom in the system. In Fig. 4(a), we illustrate the energy diagram of Mn- d states in the minority spin channel. Due to the interaction with neighboring As atoms, the $Mn-d_{yz}$ state is lower in energy than the others. This state has four lobes, two extend toward the As underneath whereas two form dangling bonds in the same vertical plane. This results in an image that has a node right above Mn and two maxima over As in the horizontal plane of view, as displayed in Fig. 4(b).

In conclusion, density functional calculations revealed interesting segregation behaviors for Mn monomer on

GaAs(110). It is shown that Mn prefer the T_{Ga} site but remain rather mobile along the trench, a result which is very important for understanding the growth and diffusion dynamics of (Ga,Mn)As. Peculiar electronic and magnetic properties, especially the extraordinary STM patterns predicted here, deserve experimental verifications. Understanding in interaction between Mn and GaAs from different perspectives is necessary for the establishment of a more comprehensive picture that describes the magnetic ordering in innovative spintronics materials.

This work was supported by the (U.S.) Department of Energy Grant No.DE-FG02-05ER46237 and Interdisciplinary Center of Theoretical Studies (ICTS). J.X.C. was supported by the National Science Foundation of China (No. 10447132), China Postdoctoral Science Foundation (No. 2004036085), K.C. Wong Education Foundation, and partly by the Science and Technology Foundation for Younger of Hunan Province. Calculations were conducted on the HP-SC45 Sigma-X parallel computer of Institute of Theoretical Physics, ICTS, and the Chinese Academy of Sciences. X.G.G. is supported by the National Natural Science Foundation of China, the special fund for major state basic research and Chinese Academy of Sciences projects. R.Q.W. is indebted to A. Yazdani of Princeton University for stimulating discussions.

¹G. Prinz, Phys. Today **48**, 54 (1995); Science **282**, 1660 (1998); J. Magn. Magn. Mater. **200**, 57–68 (1999).

²I. Malajovich, J. J. Berry, N. Samarth, and D. D. Awschalom *et al.*, Nature (London) **397**, 139 (1999); Nature (London) **411**, 770 (2001).

³H. Ohno, Science **281**, 951 (1998); Science **291**, 840 (2001).

⁴I. Zutic, J. Fabian, and S. Das Sarma, Rev. Mod. Phys. **76**, 323 (2004).

⁵H. Ohno, A. Shen, F. Matsukura, A. Oiwa, A. Endo, S. Katsumoto, and Y. Iye, Appl. Phys. Lett. **69**, 363 (1996).

⁶K. C. Ku *et al.*, Appl. Phys. Lett. **82**, 2302 (2003).

⁷D. Chiba, K. Takamura, F. Matsukura, and H. Ohno, Appl. Phys. Lett. **82**, 3020–3022 (2003).

⁸D. J. Keavney, D. Wu, J. W. Freeland, E. Johnston-Halperin, D. D. Awschalom, and J. Shi, Phys. Rev. Lett. **91**, 187203 (2003).

⁹D. Wu, D. J. Keavney, Ruqian Wu, E. Johnston-Halperin, D. D. Awschalom, and Jing Shi, Phys. Rev. B **71**, 153310 (2005).

¹⁰R. Q. Wu, Phys. Rev. Lett. **94**, 207201 (2005).

¹¹K. W. Edmonds, P. Boguslawski, K. Y. Wang, R. P. Campion, S. N. Novikov, N. R. S. Farley, B. L. Gallagher, C. T. Foxon, M. Sawicki, T. Dietl, M. B. Nardelli, and J. Bernholc, Phys. Rev.

Lett. **92**, 037201 (2004).

¹²J. M. Sullivan, G. I. Boishin, L. J. Whitman, A. T. Hanbicki, B. T. Jonker, and S. C. Erwin, Phys. Rev. B **68**, 235324 (2003).

¹³A. Mikkelsen, B. Sanyal, J. Sadowski, L. Ouattara, J. Kanski, S. Mirbt, O. Eriksson, and E. Lundgren, Phys. Rev. B **70**, 085411 (2004).

¹⁴S. C. Erwin and A. G. Petukhov, Phys. Rev. Lett. **89**, 227201 (2002).

¹⁵A. M. Yakunin, A. Yu. Silov, P. M. Koenraad, J. H. Wolter, W. Van Roy, J. De Boeck, J.-M. Tang, and M. E. Flatte, Phys. Rev. Lett. **92**, 216806 (2004).

¹⁶D. Kitchen, A. Richardella, and A. Yazdani, J. Supercond. **18**, 23 (2005).

¹⁷J. Masek and F. Maca, Phys. Rev. B **69**, 165212 (2004).

¹⁸J. X. Cao, X. G. Gong, and R. Q. Wu (to be published).

¹⁹The energy difference between T_{Ga} and T_{As} sites, 0.36 eV, indicates that the opportunity for Mn resides on T_{Ga} is about 3 times larger than that on T_{As} at room temperature according to the Boltzmann distribution.

²⁰A. Ishii, T. Aisaka, J. W. Oh, M. Yoshita, and H. Akiyama, Appl. Phys. Lett. **83**, 4187 (2003).